Hindawi
Cellular Microbiology
Volume 2022, Article ID 9854449, 19 pages
https://doi.org/10.1155/2022/9854449

Research Article

Chlamydia pneumoniae Interferes with Macrophage Differentiation and Cell Cycle Regulation to Promote Its Replication

Eveliina Taavitsainen-Wahlroos[1], **Ilkka Miettinen**[1], **Maarit Ylätalo**[1], **Inés Reigada**[1], **Kirsi Savijoki**[2], **Tuula Anneli Nyman**[3] and **Leena Hanski**[1]

[1]*Drug Research Program, Division of Pharmaceutical Biosciences, Faculty of Pharmacy, University of Helsinki, Helsinki, Finland*
[2]*Department of Food and Nutrition, Faculty of Agriculture and Forestry, University of Helsinki, Helsinki, Finland*
[3]*Department of Immunology, University of Oslo and Oslo University Hospital, Norway*

Correspondence should be addressed to Leena Hanski; leena.hanski@helsinki.fi

Received 16 December 2021; Revised 3 March 2022; Accepted 18 March 2022; Published 11 April 2022

Academic Editor: Barbara Kahl

Chlamydia pneumoniae is a ubiquitous intracellular bacterium which infects humans via the respiratory route. The tendency of *C. pneumoniae* to persist in monocytes and macrophages is well known, but the underlying host-chlamydial interactions remain elusive. In this work, we have described changes in macrophage intracellular signaling pathways induced by *C. pneumoniae* infection. Label-free quantitative proteome analysis and pathway analysis tools were used to identify changes in human THP-1-derived macrophages upon *C. pneumoniae* CV6 infection. At 48-h postinfection, pathways associated to nuclear factor κB (NF-κB) regulation were stressed, while negative regulation on cell cycle control was prominent at both 48 h and 72 h. Upregulation of S100A8 and S100A9 calcium binding proteins, osteopontin, and purine nucleoside hydrolase, laccase domain containing protein 1 (LACC1) underlined the proinflammatory consequences of the infection, while elevated NF-κB2 levels in infected macrophages indicates interaction with the noncanonical NF-κB pathway. Infection-induced alteration of cell cycle control was obvious by the downregulation of mini chromosome maintenance (MCM) proteins MCM2-7, and the significance of host cell cycle regulation for *C. pneumoniae* replication was demonstrated by the ability of a cyclin-dependent kinase (CDK) 4/6 inhibitor Palbociclib to promote *C. pneumoniae* replication and infectious progeny production. The infection was found to suppress retinoblastoma expression in the macrophages in both protein and mRNA levels, and this change was reverted by treatment with a histone deacetylase inhibitor. The epigenetic suppression of retinoblastoma, along with upregulation of S100A8 and S100A9, indicate host cell changes associated with myeloid-derived suppressor cell (MDSC) phenotype.

1. Introduction

The respiratory pathogen *Chlamydia pneumoniae* is a phylogenetically distinct, obligate intracellular gram-negative bacterium. It causes 5–10% of community-acquired pneumonia cases globally and is also associated with a high degree of mild and subclinical respiratory tract infections [1]. With a seroprevalence of 60-80% in the adult Western population, *C. pneumoniae* is the most prevalent chlamydial pathogen in humans. Besides acute respiratory infections, *C. pneumoniae* has been related to the etiology and progression of many chronic inflammatory diseases, such as atherosclerosis and asthma [2, 3]. The tendency of *C. pneumoniae* to persist inside its host cells, particularly in peripheral blood mononuclear cells (PBMCs), contributes crucially to this connection.

C. pneumoniae has a unique life cycle, where the infective elementary body (EB) and the replicative reticulate body (RB) forms alternate [4]. Under external stress factors, the productive replication cycle may be interrupted, and the bacterium may enter a metabolically altered, nonreplicative state referred to as chlamydial persistence [5]. The

morphological hallmark of this phenotype, known as the aberrant body (AB), is typically an enlarged and pleomorphic cell resulting from discontinued binary fission. This chlamydial stress response yields a viable but noncultivable bacterial phenotype that lacks infectious progeny EB production and demonstrates tolerance to standard-of-care antibiotics [6, 7]. These features contribute to marked challenges in eradicating the infection, which translate into treatment failures and recurrent infections in the clinic.

Several factors have been described to induce chlamydial persistence in in vitro models. These include β-lactam antibiotics, interferon γ (IFN-γ), γ and iron depletion [5, 8, 9]. In monocytes and macrophages, *C. pneumoniae* enters persistence spontaneously even in the absence of external triggers [10, 11]. Comparative studies on different cell culture models for *C. pneumoniae* persistence have revealed the differential regulation of both chlamydial and host cell genes depending on the persistence trigger [12, 13]. These findings highlight the heterogenous nature of chlamydial persistence. The host-bacterium interplay is probably best understood in the context of IFN-y-induced persistence [14, 15], where changes in tryptophan metabolism as well as long-term alterations in host cell apoptotic and cell cycle pathways are observed.

A well-described feature of *C. pneumoniae* infection is the induction of a proinflammatory phenotype in the host cell. *C. pneumoniae*-infected monocytes and macrophages produce different cytokines such as TNF-α [16] and the interleukins IL-6, IL-8, and IL-12 [17, 18]. The induction of surface proteins such as ICAM-1, in turn, promotes the transendothelial migration of *C. pneumoniae*-infected peripheral blood mononuclear cells [19, 20]. The bacterium has also been reported to affect leukocyte maturation, inducing the differentiation of infected monocytes into macrophages [20] and affecting dendritic cell polarization [21]. Yet another manifestation of the proinflammatory consequences of macrophage infection is their lipid and redox dysregulation, leading to macrophage conversion to foam cells [22, 23].

As illustrated above, several studies have addressed *C. pneumoniae*–PBMC interactions in terms of how the infection triggers pathological changes in the host cells. The infection-induced Toll-like receptor (TLR)-mediated signaling plays a central role in these events. However, the factors involved in the bacterial phenotypic switch resulting in *C. pneumoniae* persistence in peripheral blood mononuclear cells are less understood.

Transcriptome-wide gene expression changes in *C. pneumoniae*-infected mononuclear cells have been previously evaluated [24]. However, the overall poor correlation of mRNA levels and protein quantities in a biological system is well acknowledged [25, 26]. The *C. pneumoniae* infection is likely to alter host cell protein accumulation and thus results in events not captured by transcriptional analysis. To date, host cell proteomic profiles of *C. pneumoniae* infection have been studied solely in permissive epithelial cells by 2D-PAGE analysis [27]. The persistent infection seen in monocytes and macrophages is likely associated with very different host responses, but this has not been studied at the proteome level. Here, we used high-resolution, label-free quantitative mass spectrometry (MS)-based proteomics analysis to shed light on this host-pathogen interplay.

Given the current challenges in detecting and treating persistent *C. pneumoniae* infections, there is an urgent need for the elucidation of chlamydial persistence mechanisms and their interaction with host innate immune system cells to identify biomarkers and new potential drug targets. The tendency of *C. pneumoniae* to persist in monocytes and macrophages even in the absence of exogenous triggers is well known, but the underlying host-chlamydial interactions remain elusive. In this work, we have described changes in macrophage intracellular signaling pathways induced by *C. pneumoniae* infection. Based on the findings of the proteome analysis, infection-related responses in host cell cycle G1 to S transfer stage mediators were studied. Within the follow-up analysis, we observed the role of cell cycle regulation in altering the chlamydial phenotype and the ability of *C. pneumoniae* to interfere with macrophage differentiation.

2. Materials and Methods

2.1. Cell Culture. All cell cultures were maintained at 37°C, 5% CO2, and 95% air humidity throughout the subculture. THP-1 cells (ATCC TIB-202; ATCC, Manassas, VA, USA) were maintained in RPMI 1640 Dutch modification medium (Gibco, Thermo Fisher Scientific, Waltham, MA, USA) supplemented with 10% fetal bovine serum (FBS) (BioWhittaker, Lonza, Basel, Switzerland), 2 mM L-glutamine (BioWhittaker), 0.05 mM mercaptoethanol (Gibco, Thermo Fisher Scientific, Waltham, MA, USA), and 20 μg/ml gentamicin (Sigma-Aldrich, St. Louis, MO, USA). Hep-2cells (ATCC CCL-23) were maintained in DMEM (Gibco, Thermo Fisher Scientific) supplemented with 10% FBS and 20 μg/ml gentamicin.

2.2. C. Pneumoniae Infection. For differentiation into macrophage-like cells, THP-1 cells were seeded onto 6-well plates (density 1×10^6 cells per well) or 24-well plates (infectious progeny assays, 3.5×10^5 cells per well) and incubated for 72 h with 0.16 μg/ml phorbol-12-myristate-13-acetate (PMA) (Sigma-Aldrich, St. Louis, MO, USA). The resulting confluent monolayer was inoculated with *C. pneumoniae* (strain CV6, a cardiovascular isolate obtained from Professor Matthias Maass, Paracelsus Medical University, Salzburg, Austria) and propagated as previously described [28] at a multiplicity of infection (MOI) 3 or 1 (infectious progeny assays). To synchronize the infection, the plates were centrifuged at 550×*g* for 1 h and further incubated 1 h in 37 °C. Then, fresh medium was added, and the cultures were incubated for the indicated times (24–144 h) before collecting samples for the analyses described below.

2.3. Growth Kinetics and Infectious Progeny Assays. C. pneumoniae growth kinetics and infectious progeny production in THP-1 macrophages was determined as previously described [29]. Shortly, in kinetic assays, THP-1 macrophages were infected as described above, and culture lysates were collected at various time points and total cellular DNA

was extracted with a GeneJET Genomic DNA Purification Kit (Thermo Fisher Scientific). *C. pneumoniae* genome copy numbers were quantified as based on the ompA gene, using StepOnePlus Real-Time PCR System (Thermo Fisher Scientific).

For infectious progeny determination, the EBs were harvested from infected THP-1 macrophages from 24-well plates at 72–144-h postinfection by lysing the host cells. The bacterial progeny was quantified by inoculating Hep-2 cell monolayers with the THP-1 cell lysates and culture supernatant. Chlamydial growth was determined based on the chlamydial inclusion counts observed in Hep2 monolayers by staining with a genus-specific anti-LPS antibody (Pathfinder Chlamydia Culture Confirmation System, Bio-Rad) after 72-h incubation using the Invitrogen™ EVOS® FL Imaging System (Thermo Fischer Scientific).

2.4. Protein Extraction and Purification. At 48-h and 72-h postinfection, THP-1 macrophages were washed with Tris buffer 100 mM, pH 7.2–7.4, and carefully suspended from the wells by a cell scraper into 1 ml of the same Tris buffer. The cells were centrifuged at 200×*g* for 5 min by ultracentrifuge (Heraeus Fresco 21 Centrifuge, Thermo Fisher Scientific). After centrifugation, the supernatants were discarded, and the pellets were stored at -80 ˚C.

The cells were suspended in 50 μl of 0.1% RapiGest™ SF (Waters, Milford, MA, USA) in 100 mM triethylammonium bicarbonate; pH 8.5 (TEAB, Thermo Fisher Scientific) with three spoonfuls (ca 30 μl) of 0.1-mm glass beads (Sigma Aldrich) were homogenized by FastPrep-24 (MP Biomedicals) with motor speed set at 6.5 three times for 20 sec. Samples were kept on ice between the cycles. The cell-free supernatants with soluble proteins were obtained by centrifuging (16 000×*g*, 3 min). Additional 100 μl of RapiGest was added to the supernatants to optimize the protein concentration for in-solution digestions.

After a 45-min incubation on ice, the protein disulfide bonds were reduced with 10 mM DL-dithiothreitol (Sigma-Aldrich) for 45 min at 60 ˚C and alkylated with 15 mM iodoacetamide (Sigma-Aldrich) for 60 min at RT (in dark). Finally, 20 mM DL-dithiothreitol was added to quench the extra iodoacetamide. Thirty-μg aliquots of protein were taken as based on spectrophotometric concentration determination using the Multiskan Sky Microplate Spectrophotometer (Thermo Fisher Scientific) and diluted with 100 mM TEAB to a final volume of 50 μl. Sequencing grade modified trypsin (Promega, Madison, WI, USA) was added in 1 : 60 enzyme-to-protein ratio, and the samples were digested at 37 ˚C for 17 h. The digestion was stopped, and the RapiGest precipitated by adding 0.5% trifluoroacetic acid (37 ˚C for 40 min). The tryptic peptides were collected by centrifugation (20 000×*g* for 5 min); the peptides were purified/concentrated using ZipTip C18 (Merck Millipore, Burlington, MA, USA) and evaporated to dryness.

2.5. Label-Free Quantitative Proteome Analysis. The peptides were dissolved in 0.1% formic acid and analyzed by nanoLC-MS/MS using nEASY-LC coupled to Q Exactive Plus with 25 cm EASY-Spray PepMap®RSLC column and 120 min separation gradient. For protein identification and label-free quantification, the LC-MS/MS data were searched with MaxQuant v. 1.6.1.0 against UniProt human (Sept 2018), CV6, and CV14 databases. The sequencing of the CV6 isolate was carried out at the Institute of Biotechnology at the University of Helsinki. The CV14 database was annotated using NCBI BLAST [30]. The CV6 genome has been shown to be highly similar with the previously sequenced cardiovascular *C. pneumoniae* CV-14 [31]. Additional data processing and statistical analysis was performed using Perseus v. 1.6.7.0. The mass spectrometry proteomics data have been deposited to the ProteomeXchange Consortium via the PRIDE [1] partner repository with the dataset identifier PXD030232.

2.6. Bioinformatics and Statistical Analysis. Three biological replicates were analyzed. Proteins quantified in at least 2 out of 3 replicates in at least one sample group were considered valid and included in the bioinformatics analysis. Missing values were imputed by random draws from a low-abundance-adjusted normal distribution using the Perseus software v. 1.6.7.0 [32].

A one-way ANOVA with a false discovery rate (FDR) of 0.10 was carried out in Perseus to identify proteins with differential expression between any of the conditions and time points. These proteins were subjected to hierarchical clustering. LFQ protein abundances were compared between non-infected and infected THP-1 cells at different time points by Student's *t*-test with a permutation-based FDR of 0.05.

Statistically significant proteins from ANOVA were included in canonical pathway analysis using the Ingenuity Pathway Analysis software (2000-2019 IPA; QIAGEN Silicon Valley, Redwood, CA, USA) and STRING Functional Enrichment Analysis database v. 11 [33].

2.7. RT-PCR. For RT-PCR analysis, cells were infected in 6-well plates as described above. Samples were collected at 48-h postinfection. Cells were scraped from the plate and total RNA was extracted using PureLink RNA mini kit (Thermo Fischer Scientific). cDNA was synthetized right after RNA purification using RevertAid First Strand cDNA Synthesis Kit (Thermo Fisher Scientific). Purified RNA was used as a template for cDNA synthesis.

The expression of selected genes was quantified with Step One Plus™ Real-Time PCR system using specific human cDNA primers (Supplementary Table 1), and the obtained values were normalized to glyceraldehyde 3-phosphate dehydrogenase (GAPDH) as an endogenous reference gene. The Ct values were calculated using the $2^{-\Delta\Delta Ct}$ equation. For the evaluation of histone deacetylases in *C. pneumoniae*-induced downregulation of retinoblastoma (Rb) protein, valproic acid was purchased from Tocris Bioscience (United Kingdom).

2.8. Western Blot. THP-1 macrophages were infected as described above with MOI 3. When analyzing total and phosphorylated retinoblastoma protein levels, treatment with 100 nM Palbociclib, a selective inhibitor for cyclin-dependent kinase 4 (CDK4) and 6 (CDK6) (Sigma-Aldrich),

was applied as control. The cells were collected by scraping at 48-h postinfection and lysed in cold RIPA buffer (150 mM NaCl, 1% NP40, 0.5% sodium deoxylate, 0.1% sodium dodecyl sulfate, and 25 mM Tris in water supplemented with Pierce phosphatase inhibitor and Pierce protease inhibitors) (Thermo Fisher Scientific). Insoluble material was separated by centrifugation at 13800×*g* for 20 min. The supernatants were stored at -80°C.

Total protein concentrations of the samples were determined with BCA protein assay (Thermo Fisher Scientific) and detected with Multiskan Sky plate reader (Thermo Fisher Scientific). Equal amount of protein was suspended with 4× Laemmli sample buffer (Bio-Rad, Hercules, California, USA) and denatured by heating at 95°C, 5 min. Samples were loaded into SDS-PAGE (TGX stain-free gel, Bio-Rad), and separated proteins were transferred into a nitrocellulose membrane (Bio-Rad). The total Rb amount of the samples was determined using polyclonal rabbit IgG antibody (PA5-27215, Thermo Fisher Scientific), and Rb ser608 and 780 phosphorylation was determined using polyclonal rabbit IgG antibodies (PA5-104642 and 701272, respectively, both from Thermo Fisher Scientific). S100A9 (D5O6O), NF-κB2 p100/p52, and GAPDH (14C10) antibodies were obtained from Cell Signaling Technology (Massachusetts, USA). HRP-conjugated goat anti-rabbit IgG secondary antibody was obtained from Thermo Fischer Scientific. The blots were analyzed using ChemiDoc imaging system and ImageLab 6.0 software (Bio-Rad) and normalized to the total protein amount of each gel.

3. Results and Discussion

3.1. C. pneumoniae Infection Phenotype in THP-1 Macrophages. The phenotype and behavior of *C. pneumoniae* infection vary remarkably depending on the host cell line and bacterial strain [34–36]. Monocytic and macrophage cell lines have been reported to support the growth of some *C. pneumoniae* strains but with limited *C. pneumoniae* replication [10, 24, 36, 37].

According to our previous data, *C. pneumoniae* cardiovascular isolate CV6 infection in THP-1 monocyte-derived macrophages results in a mixed infection phenotype with simultaneously present productive and persister subpopulations [29]. As described by Daigneault et al. [38], THP-1 cells undergoing growth arrest and macrophage differentiation share transcriptional profiles similar to primary monocytes undergoing terminal differentiation, which is further enhanced during subsequent days after PMA removal. This infection model, representing a spontaneously rising subpopulation of persistent *C. pneumoniae* cells inside macrophages undergoing terminal differentiation, was characterized in the present work by qPCR, quantitative culture, and antibiotic susceptibility studies.

In the qPCR analysis, an increase in genome numbers, indicative of a bacterial subpopulation undergoing DNA replication, was observed after a MOI 3 infection of the macrophages (Figure 1(a)).

Earlier work indicates that *C. pneumoniae* persistence may involve bacterial DNA replication even in the absence of cell division, and it was thus of interest to study whether infectious *C. pneumoniae* progeny was also generated in the infected macrophages. Productive infection was confirmed by passaging the infected macrophage cell lysates, and culture supernatants collected 72–144-h postinfection onto permissive epithelial cell monolayers. All samples collected from infected macrophage cultures were culture positive, the total number of inclusion forming units per ml (IFU/ml) at 72-h postinfection being, on average, 210,000 in macrophage lysate samples and 16,000 in supernatant samples.

In macrophage cell lysates, the number of detected IFUs rose sharply between 96-h and 120-h postinfection and stayed at a similar level at 144 h (Figure 1(b)). In the supernatant samples, the number of chlamydial progeny EBs increased steadily throughout the observation time, indicating that matured EBs were readily able to leave the primary host cell to infect others. Between 72-h and 144-h postinfection, the EB number tripled or quadrupled in supernatant samples and cell lysates, respectively.

Based on these data, the active replication and infectious progeny production of *C. pneumoniae* in PMA-differentiated THP-1 macrophages were confirmed. To further evaluate the infection characteristics in THP-1 derived macrophages, an antibiotic susceptibility test was carried out using azithromycin, the golden standard for treating chlamydial infections, by determining its effect on *C. pneumoniae* EB progeny production in these cells. While azithromycin's chlamydicidal effect in permissive cell lines is achieved at approximately 20 nM [39], we did not observe any inhibition of *C. pneumoniae* EB production with 20 nM azithromycin in the THP-1-derived macrophages (data not shown). Even at 200 nM, azithromycin treatment did not clear the macrophage cultures from infectious *C. pneumoniae* progeny (Figure 2), implying significantly increased azithromycin tolerance. Clearance of infection was noticed with 1 μM concentration, on not clinically relevant concentration [40]. We have previously described that *C. pneumoniae* eradication by azithromycin in THP-1-derived macrophages can be enhanced by a redox-active small molecule that promotes chlamydial EB production [29]. These findings indicate that the antibiotic susceptibility of *C. pneumoniae* in the macrophages can be altered by promoting productive infection.

Collectively, these observations imply that the THP-1-derived macrophages harbor both productively replicating and persistent *C. pneumoniae* populations while suggesting that the balance between the two coexisting bacterial populations is governed by factors within the intracellular environment. Shedding light on the nature of these factors would illuminate the molecular details of *C. pneumoniae*–macrophage interactions and guide us towards a rational therapy design for eradicating persistent infections.

3.2. Changes in the Host Cell Proteome upon C. pneumoniae Infection. To characterize macrophage responses during *C. pneumoniae* infection, total proteomes of infected and non-infected THP-1 cell lysates were subjected to high-resolution LC-MS/MS analysis and label-free quantification. Based on

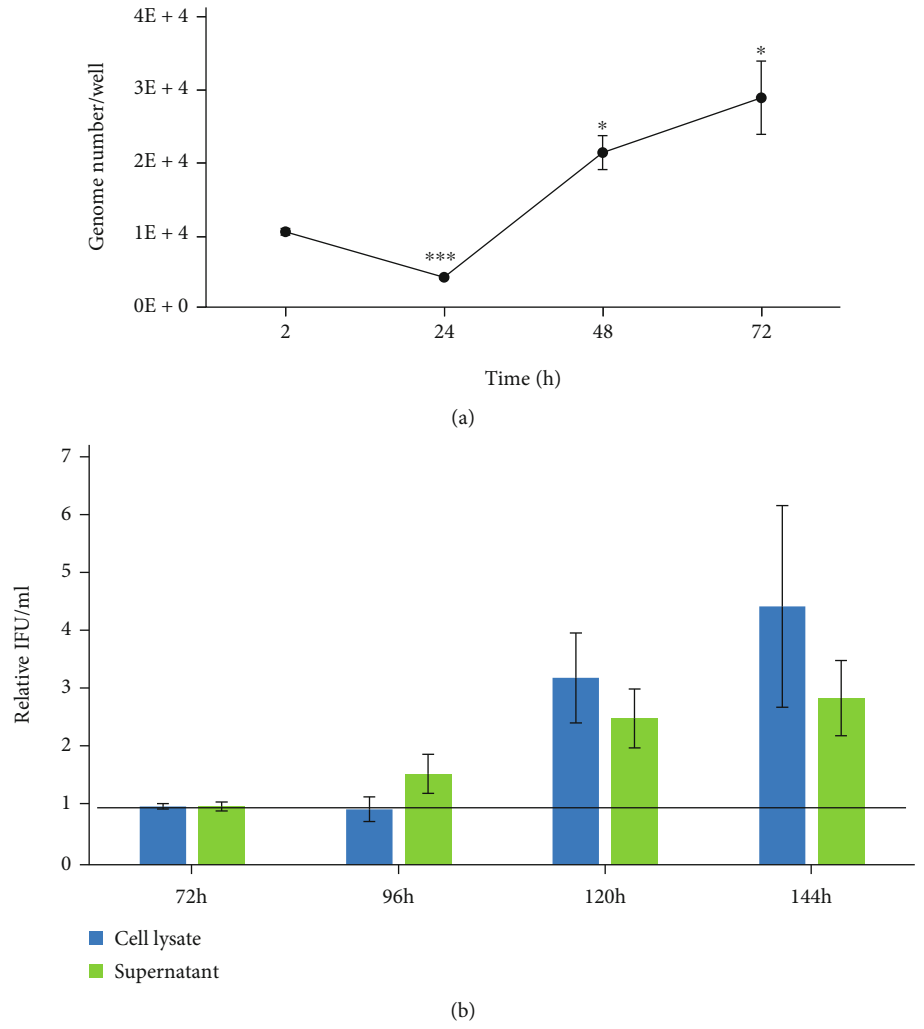

Figure 1: *C. pneumoniae* growth kinetics and progeny production in THP-1 macrophages. (a) *C. pneumoniae* growth kinetics in THP-1 macrophages. Cells were infected at MOI 3 IFU/cell, and *C. pneumoniae* genome copy numbers were determined by qPCR on ompA gene. Data are shown as total genome number of *C. pneumoniae* per well ± SEM ($n = 4$). Statistical analyses were made by IBM SPSS statistics 25 software. Differences between means were calculated with Student's *t*-test with Bonferroni correction, and significance is presented as marks of *p* values compared to 2-h genome number: <0.05: ∗; <0.01: ∗∗; and <0.001: ∗∗∗. (b) Quantification of infectious *C. pneumoniae* EBs following an infection of THP-1 macrophages. Permissive epithelial cells were inoculated with cell lysates from THP-1 macrophages or supernatant from culture medium of infected THP-1 macrophages collected at 72-h, 96-h, 120-h, or 144-h postinoculation. *C. pneumoniae* inclusion counts after immunofluorescence staining of the monolayers were determined and converted to IFU/ml. Data are presented as IFU/ml values normalized to the value 72 h after infection and shown as mean ± SEM ($n = 4$). No statistical significance was noticed.

the kinetic analysis of the infection (Figure 1) and earlier transcriptomics data [24], we focused on time points representing a readily established stage of infection and proceeded to isolate proteins at 48-h and 72-h postinfection. In *C. pneumoniae* life cycle, 48 h after inoculation represents a stage of the active bacterial replication period based on the literature [15] and the replication results presented in this paper, while maturation of the first EBs occurs approximately at 72-h postinfection. Monocyte transcriptomics also indicates that the innate responses arising from recognition of *C. pneumoniae* molecular patterns by monocytic pattern recognition receptors are diminished or stabilized by 48 h [24]. Thus, the infection-induced changes in host cell proteomes starting from thereon is expected to be more representative for the adaptation to a long-lasting infection.

In proteome analysis, we identified approx. 3000 proteins and obtained reliable quantification data from 2136 proteins, all of them being of host cell origin (Supplementary Table 2).

Principal component analysis was carried out based on these quantifications. Infection status appeared to be the main factor separating the sample profiles regardless of the time point (Figure 3(a)), although two possible outliers (condition1 and condition2) were noticed. A one-way ANOVA (permutation-based FDR 0.10) identified a substantial number of proteins with significantly and consistently altered

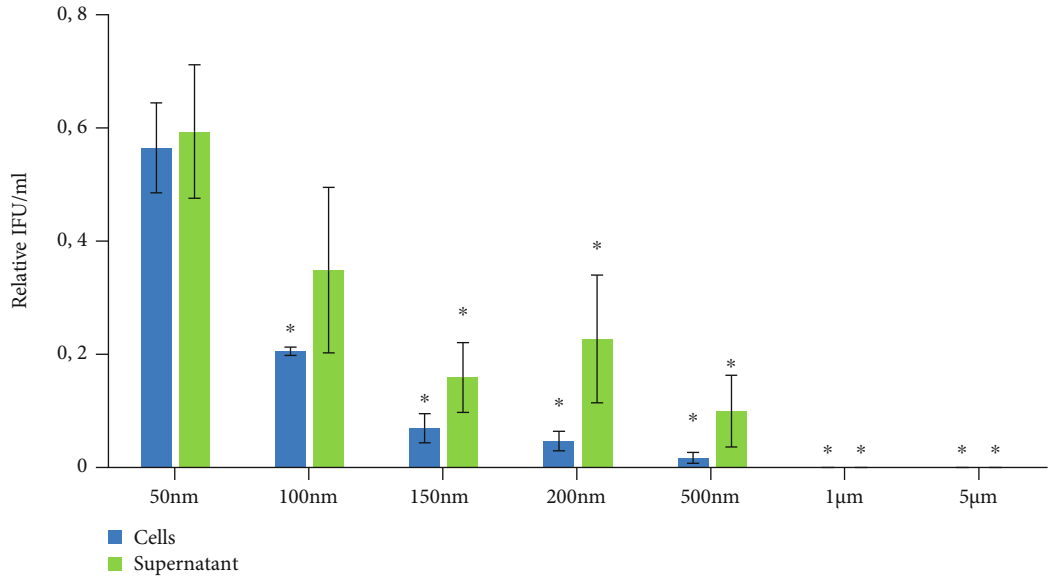

Figure 2: Inhibition of *C. pneumoniae* infectious progeny production by azithromycin in THP-1 macrophages 72-h postinfection. Results are presented as inclusion forming units/ml normalized to the mock infection and shown as mean ± SEM, MOI 3 infection ($n = 4$). Statistical analysis was made by IBM SPSS statistics 25 software. Differences between means were calculated with Student's t-test with Bonferroni correction, and significance is presented as marks of P values compared to nontreated infection control: <0.05:∗.

expression between the conditions and time points ($n = 214$), thus warranting the continued inclusion of all replicate samples in the analyses. These proteins were subjected to further biostatistics and bioinformatics investigations to characterize the effect of *C. pneumoniae* infection in the macrophages at different stages of infection.

A hierarchical clustering was conducted to illustrate general protein abundance trends arising from the infection and culture time. As with the PCA, *C. pneumoniae* infection appeared to be the most important factor separating the samples, although time point-specific trends were additionally observed (Figure 3(b)). Differential expression within these proteins by time point and infection status was further studied by unpaired Student's t-test, where 1.5 or higher fold change and q-value ≤0.05 were considered as a statistically significant result. Numbers of proteins showing statistically significant difference between *C. pneumoniae*-infected and noninfected samples are presented in Figure 3(c).

3.3. Pathway Analysis on C. pneumoniae-Induced Changes in Macrophage Proteome. Pathway analyses utilizing software STRING and Ingenuity Pathway Analysis (IPA) were carried out to identify infection-regulated pathways in the macrophages. The top canonical pathways recognized by the two bioinformatics tools are presented in Figure 4 and graphical summaries of the Ingenuity Pathway Analysis are shown in Supplementary Figure 1.

In *C. pneumoniae*-infected cells, a value-based STRING analysis revealed the enrichment of biological processes related to host cell response to bacterial infection at 48-h postinfection, as based on Gene Ontology (GO) annotations [41, 42]. Controlling of the cell cycle was enriched in both time points, while at 48 h the most enriched processes included leukocyte aggregation, inflammatory response, and positive regulation of NF-κB transcription factor activity. On the other hand, no such infection responses were significantly enriched at 72-h postinfection, as instead all the top 10 most enriched GO biological processes were related to cell cycle and DNA replication, which were negatively affected by *C. pneumoniae*. Hence, the active infection response phenotype appears to be dampened towards the latter time point.

Similar pathways were recognized also in IPA, although the variation between time points was less prominent than in the corresponding STRING analyses. Most of the top canonical pathways recognized by IPA, such as the inflammasome and leukocyte extravasation signaling pathways, were positively or inconsistently affected by the infection. The negatively affected cell cycle control was also recognized as one of the most significantly enriched pathways in the IPA analyses of both time points. In addition to the pathway enrichments shared between the two analysis platforms, IPA also recognized the sirtuin signaling pathway and HOTAIR regulatory pathway. The proteins identified in the negatively affected sirtuin signaling pathway were involved in the regulation of sirtuin 1 and 3 cascade reactions. Sirtuins are NAD +-dependent class III histone deacetylase enzymes known to regulate diverse cellular processes such as DNA repair, insulin sensitivity, fatty acid oxidation, inflammation, and aging [43]. The knowledge about the role of sirtuins in innate immune responses is still limited, and no published data in the context of *C. pneumoniae* infection is currently available.

IPA analyses determinate the overlap number of the described pathway. It indicates the coverage of the total pathway by the discovered proteins in samples. In the analyses, most covered pathways were inflammasome pathway, cell cycle controlling, and fatty acid β-oxidation in both time points.

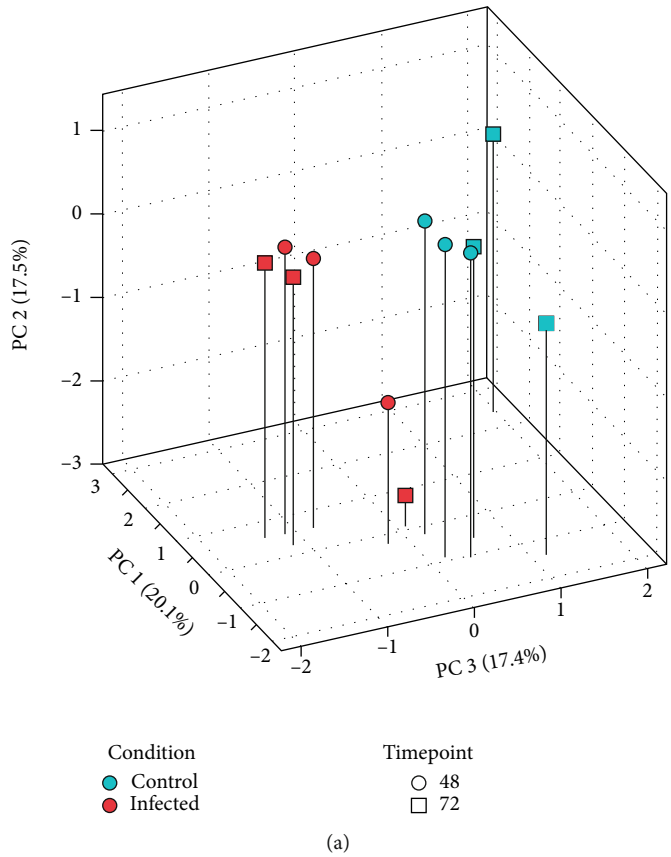

(a)

Figure 3: Continued.

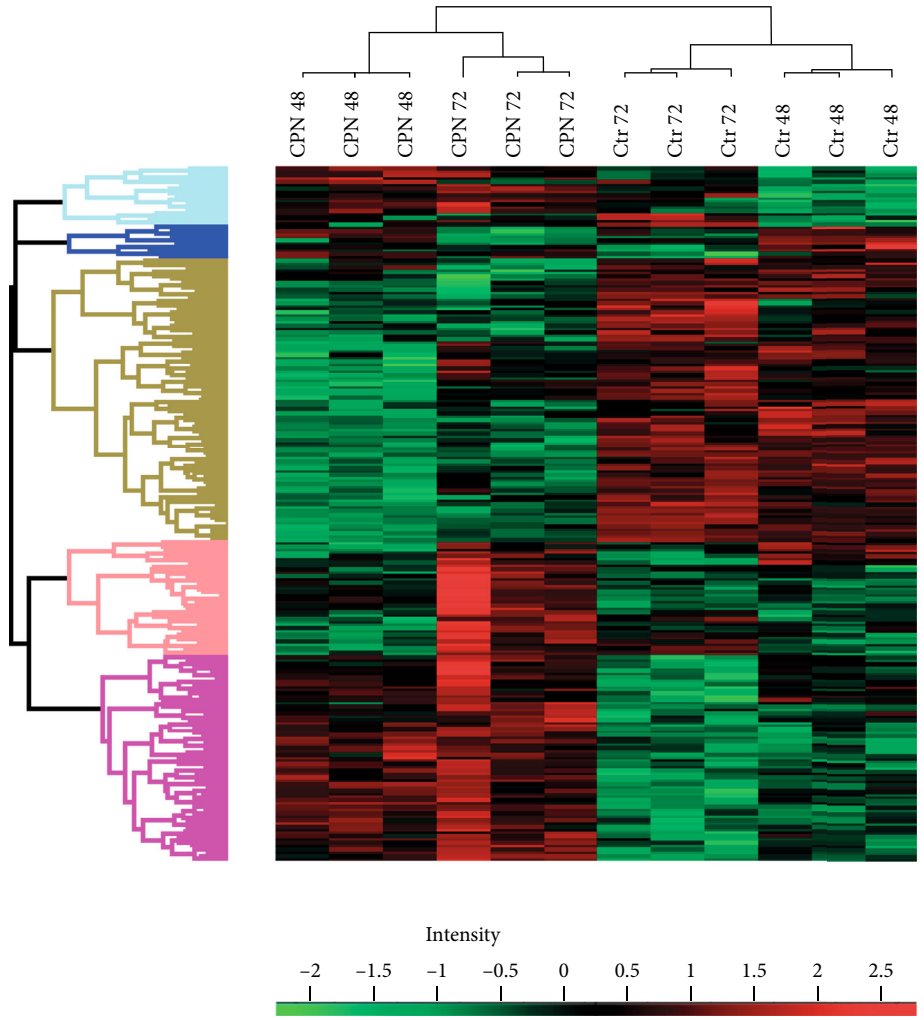

(b)

	48h		72h	
	Up	Down	Up	Down
No cut-off	96	99	96	117
Cut off 1,5-fold change	44	9	42	18

(c)

Figure 3: (a) Principal component analysis for the imputed dataset. Carried out in Perseus v. 1.6.7.0. (b) Heatmap visualizing proteins upon hierarchical clustering based on Z-scores. Red = expressed more than average; green = expressed less than average. Results presented as LFQ values normalized by z-score. (c) Numbers of proteins showing statistically significant difference between *C. pneumoniae*-infected and noninfected samples. Numbers are presented as results from pairwise comparisons with Student's *t*-test. Abbreviations: CPN = *C. pneumoniae*-infected samples; ctr = noninfected samples in different time points.

3.4. Up and Downregulated Proteins. To gain a molecular level insight into the macrophage proteome changes induced by the infection, sets of individual proteins showing most prominently differential expression between infected and noninfected cells were next evaluated. Up- and downregulated proteins at 48-h and 72-h postinfection with at least ±1.5-fold change are presented in Table 1.

3.4.1. Upregulated Proteins. As expected, proteins associated with leucocyte activation and inflammation were abundant among the upregulated proteins in the infected samples. Consistent with previous reports [44], *C. pneumoniae* infection increased Toll-like receptor 2 (TLR2) expression in the macrophages. Chlamydial heat shock protein 60 has been shown to activate TLR2 and TLR4 receptors [45]. Activation of TLR2 receptors can lead to many different pathways in the host cells during infection, including the induction of NF-κB. The role of TLR2 in *C. pneumoniae*-induced pathology has also recently been demonstrated in atherosclerosis development [46]. Besides TLR2, another innate immunity receptor, CD14 exhibited significant upregulation in the infected cells. CD14 is a membrane protein initiating the signaling cascade responsible for the LPS of gram-negative bacteria. Despite their central role in innate immunity, both

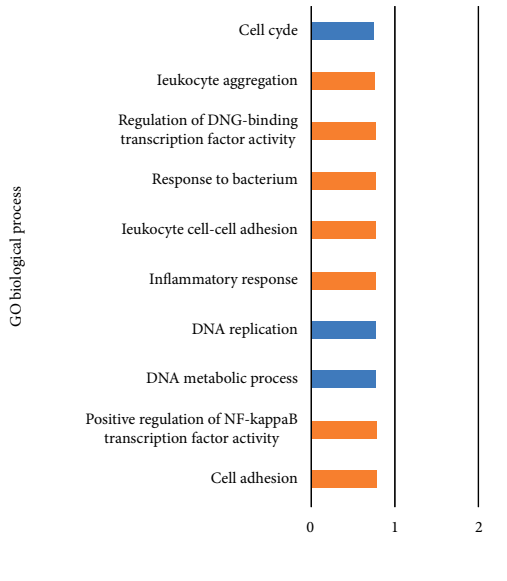

Pathway	*P*-value	Overlap
Cell cycle control of chromosomal replication ∗	3.31×10^{-9}	14.3%
Sirtuin signaling pathway ↓	4.10×10^{-6}	3.77%
Leukocyte extravasation signaling ↑	7.10×10^{-6}	4.55%
Fatty acidβ-oxidation I ○	5.74×10^{-5}	12.5%
HOTAIR regulatory pathway ↑	9.32×10^{-5}	4.40%
Remodeling of epithelial adherens junctions ○	9.55×10^{-5}	7.25%
Inflammasome pathway ○	2.95×10^{-4}	15.0%
Phagosome maturation ∗	5.01×10^{-4}	4.00%
Osteoarthritis pathway ↑	5.50×10^{-4}	3.29%
Autophagy ○	7.24×10^{-4}	6.56%

(a)

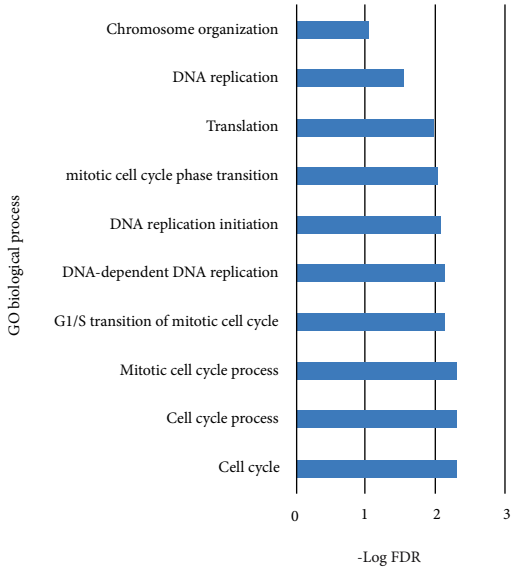

Pathway	*P*-value	Overlap
Sirtuin signaling pathway ↓	4.14×10^{-9}	5.48%
Cell cycle control of chromosomal replication ∗	2.26×10^{-8}	14.3%
Inflammasome pathway ↑	2.16×10^{-5}	20.0%
Leukocyte extravasation signaling ↑	4.96×10^{-5}	4.55%
Osteoarthritis pathway ↑	8.70×10^{-5}	4.23%
Fatty acidβ-oxidation I ○	1.48×10^{-4}	12.5%
Neuroinflammation signaling pathway ↑	2.45×10^{-4}	3.33%
Remodeling of epithelial adherens junctions ○	2.95×10^{-4}	7.25%
HOTAIR regulatory pathway ↑	4.17×10^{-4}	4.40%
Tryptophan degradation III(eukaryotic) ○	8.13×10^{-4}	13.6%

(b)

Figure 4: Top 10 canonical pathways showing changes in infected vs non-infected macrophages at (a) 48-h and (b) 72-h postinfection. ANOVA-filtrated protein sets with statistical difference values from *t*-test were used in analysis. Analyses were carried out using STRING Functional Enrichment Analysis v11 (left) and Ingenuity Pathway Analysis (right). Enrichment in STRING analysis according to Gene Ontology (GO) terms are presented as the false discovery rate (FDR). Orange = positive change induced by the infection; blue = negative change; ↑ = positive; Z core; ↓ = negative Z-core; ○ = Z core 0; ∗= no activity pattern available. Overlap indicates the coverage of the total pathway by the discovered proteins.

CD14 and TLR2 expression are downregulated during monocyte-to-macrophage differentiation in primary monocytes as well as in PMA-treated THP-1 cells [38]. Previous data suggest that monocyte differentiation is induced upon *C. pneumoniae* infection [20], but the current findings on CD14 and TLR2 upregulation indicate that the infection may in fact interfere with the normal macrophage maturation route and thus promote bacterial survival in these cells.

The most upregulated proteins in this study included S100A8 and S100A9, two dimer-forming calcium-binding proteins with various intracellular and extracellular functions. These proteins are suggested to be transcriptional targets of NF-κB [47] and STAT3 [48]. They are induced in monocyte-derived macrophages upon proinflammatory stimuli, but no previous reports on their connection with chlamydial infections exist [49]. Interestingly, the expression of S100A8 and S100A9 is associated with a macrophage phenotype described as proinflammatory but ineffective in *Mycobacterium* clearance [50]. Another study reports the augmented resistance of epithelial cells towards intracellular

Table 1: Differentially expressed proteins in *C. pneumoniae*-infected macrophages. (a) Upregulated and (b) downregulated proteins (LFQ fold change of ±1.5 or larger).

(a)

Protein	Accession no.	Fold change	Protein	Accession no.	Fold change
48 h			72 h		
S100A9	P06702	10.27	*S100A9*	P06702	17.05
AMPD3	Q01432	5.95	*S100A8*	P05109	8.28
LACC1	Q8IV20	5.34	*LACC1*	Q8IV20	6.90
NFKB2	Q00653	4.79	*AMPD3*	Q01432	6.56
S100A8	P05109	4.66	*ACAD10*	O14672	6.38
SPP1	P10451	4.49	*IDI1*	Q13907	5.54
CD14	P08571	4.46	*CD14*	P08571	4.29
PTPN1	P18031	4.20	*ICAM1*	P05362	3.59
ICAM1	P05362	4.07	*RTN1*	Q16799	3.45
RTN1	Q16799	4.06	*TDO2*	P48775	3.39
DDX24	Q9GZR7	3.41	*ALOX5AP*	P20292	3.38
CTNND1	O60716	3.21	*EXOSC5*	Q9NQT4	2.99
MARCKSL1	P49006	3.13	*CHCHD2*	Q9Y6H1	2.91
TMPPE	Q6ZT21	2.99	*CUX1*	P39880	2.90
SH3PXD2B	A1X283	2.66	*SELO*	P77649	2.79
IL4I1	Q96RQ9	2.44	*SH3PXD2B*	A1X283	2.76
HK2	P52789	2.34	*MARCKSL1*	P49006	2.76
NCF1	P14598	2.33	*HK2*	P52789	2.74
NAMPT	P43490	2.27	*NCF1*	P14598	2.70
TLR2	O60603	2.23	*TYMP*	P19971	2.66
TDO2	P48775	2.21	*NFKB2*	Q00653	2.61
TGFBI	Q15582	2.18	*KYNU*	Q16719	2.45
HMOX1	P09601	2.14	*SPP1*	P10451	2.26
MRPS17	Q9Y2R5	2.04	*MX1*	P20591	2.13
MX1	P20591	2.02	*NRP1*	O14786	2.13
CD44	P16070	2.01	*EHD1*	Q9H4M9	1.99
ALOX5AP	P20292	2.00	*ZFR*	Q96KR1	1.93
CD36	P16671	1.99	*COL6A1*	P12109	1.91
KYNU	Q16719	1.96	*NAMPT*	P43490	1.91
EHD1	Q9H4M9	1.87	*DENND3*	A2RUS2	1.90
NRP1	O14786	1.85	*HMOX1*	P09601	1.86
TYMP	P19971	1.82	*IL4I1*	Q96RQ9	1.80
COL6A1	P12109	1.79	*OAT*	P04181	1.78
PPIF	P30405	1.75	*PTPN1*	P18031	1.75
NQO1	P15559	1.72	*TGFBI*	Q15582	1.64
ERGIC1	Q969X5	1.70	*OAS3*	Q9Y6K5	1.62
ACSL4	O60488	1.61	*ATG7*	O95352	1.56
SELO	P77649	1.59	*NQO1*	P15559	1.55
SLC3A2	P08195	1.54	*FAM129B*	Q96TA1	1.52
CTSD	P07339	1.53	*PLEKHO2*	Q8TD55	1.51
PLEKHO2	Q8TD55	1.52	*CD44*	P16070	1.51
DENND3	A2RUS2	1.51	*HMGB3*	O15347	1.50
CSF1R	P07333	1.50			
PTPRJ	Q12913	1.50			

(b)

Protein	Accession no.	Fold change	Protein	Accession no.	Fold change
48 h			72 h		
GGT1	P19440	0.10	*GGT1*	P19440	0.34
SSBP1	Q04837	0.29	*PARP10*	Q53GL7	0.37
DCAF8	Q5TAQ9	0.32	*MCM5*	P33992	0.43
MCM6	Q14566	0.49	*MRPS17*	Q9Y2R5	0.45
FABP4	P15090	0.51	*MCM4*	P33991	0.47
MCM3	P25205	0.55	*MRPL16*	Q9NX20	0.50
MCM4	P33991	0.63	*MCM6*	Q14566	0.53
MCM5	P33992	0.63	*VAMP8*	Q9BV40	0.57
MCM2	P49736	0.66	*MCM3*	P25205	0.58
			MCM2	P49736	0.59
			SUN2	Q9UH99	0.59
			DNASE2	O00115	0.59
			FABP4	P15090	0.60
			APMAP	Q9HDC9	0.60
			CA2	P00918	0.62
			SRP9	P49458	0.62
			STMN1	P16949	0.64
			RPA1	P27694	0.66

bacteria when concomitantly transfected with both proteins [51]. We confirmed the infection-induced upregulation of S100A9 by RT-PCR (data not shown) and western blot (Supplementary Figure 2). Based on these findings, the role of S100A8/A9 heterodimers in restricting *C. pneumoniae* replication in macrophages warrants further investigation.

Purine nucleoside hydrolase, laccase domain-containing protein 1 (LACC1, also known as C13orf31 and FAMIN), was the third most upregulated protein at both time points. LACC1 is a peroxisome and endoplasmic reticulum-associated protein with the primary role of microbial clearance in peripheral macrophages [52, 53]. It is required for pattern recognition receptor (PRR)-induced mitochondrial reactive oxygen species (ROS) production, MAPK, and NF-κB pathway activation. Expression of LACC1 has been also shown to be induced upon PMA differentiation of THP-1 cells [52]. Furthermore, LPS stimulation of THP-1 macrophages leads to a further increase of LACC1 mRNA expression, which correlates with the present finding of LACC1 upregulation upon *C. pneumoniae* infection.

Osteopontin (SPP1) was upregulated 4-fold at 48-h post-infection and 2-fold at 72 h, compared to the noninfected cells. SPP1 acts as a cytokine with a key role in controlling the secretion levels of interleukins and stimulating the production of interferon-gamma [54, 55]. It is also important for macrophage adhesion and differentiation. Interestingly, SPP1 increases calcification in arteries [56] and has additionally been associated with atherosclerosis, with one possible mechanism being the increase of vascular inflammation by macrophage activation [54]. *C. pneumoniae* has been previously reported to increase the expression of SPP1 in mesothelial cells [57], and since the infection has been also connected to atherosclerosis, SPP1 could act as a link in this association.

Various studies have described the rapid activation of NF-κB upon host cell contact with *C. pneumoniae* [58]. Even though the immediate NF-κB activation was obvious by the above-mentioned downstream proteins as well as the findings from the pathway analyses, we also observed an upregulation of the inhibitory NF-κB2 protein in the infected macrophages. The infection-induced upregulation was also confirmed by western blot (Supplementary Figure 2). This polypeptide exerts classical I-κB functions by sequestering transcription activator NF-κB subunits [59]. As a key member of the noncanonical NF-κB pathway, the processing of NF-κB2 is tightly regulated and is associated with functions like tryptophan metabolism and mucosal immunity towards pathogens [60]. To the best of our knowledge, chlamydial interactions with noncanonical NF-κB signaling have not been described earlier.

The expression of the scavenger receptor CD36 was significantly upregulated by the infection. This transmembrane protein has a major role in the uptake of oxidized low-density lipoprotein (LDL), and it is considered necessary for macrophage foam cell formation [61]. Indeed, several studies have demonstrated the induction of foam cell formation by *C. pneumoniae* in vitro and in vivo [22, 62, 63]. Alterations in the expression of proteins associated with cholesterol metabolism have been reported upon infection, but changes in CD36 expression represent a novel finding in this context. Another upregulated protein related to lipid metabolism was acyl-CoA dehydrogenase family member 10 (ACAD10). It was strongly upregulated at 72-h postinfection, but no change in regulation was evident at 48-h

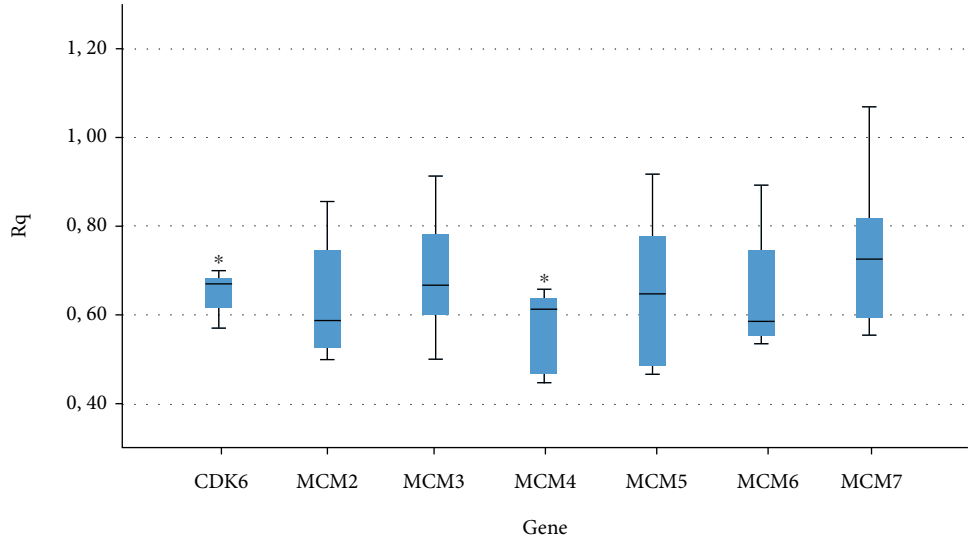

Figure 5: *C. pneumoniae* infection-induced changes in the expression of genes involved in cell cycle regulation. THP-1 macrophages were infected with MOI 3, and total RNA of the infected and noninfected control cells were collected at 48-h postinfection. After cDNA synthesis, the expression of each gene was determined by $2^{-\Delta\Delta Ct}$ method using GADPH as an internal reference gene. Data are presented as box blot of relative quantification of genes, ($n = 6$). Statistical analysis was made by IBM SPSS statistics 25 software. Differences between means were calculated with Student's t-test with Bonferroni correction. Statistical significance is presented as marks of p-value: <0.05:∗. Abbreviations: Rq = relative quantification.

postinfection. ACAD10 participates in the beta-oxidation of fatty acids in mitochondria [64], a process accelerated upon *C. pneumoniae* infection [65].

3.4.2. Downregulated Proteins. The most intensely downregulated protein in the infected vs. noninfected samples was the glutathione hydrolase 1 proenzyme, gamma-glutamyl transferase (GGT1). GGT1 is a plasma membrane-bound protein which participates in glutathione (GSH) metabolism by catabolizing extracellular GSH, thus contributing to the maintenance of intracellular GSH pools by providing building blocks for de novo GSH biosynthesis [66]. Time-dependent fluctuation in host cell GSH levels has been reported in earlier studies, and the macrophage intracellular redox milieu is suggested to play a role in governing *C. pneumoniae* infection phenotype [67, 68]. The role of GGT1 in mediating infection-driven alterations in host cell redox balance thus warrants further investigation.

Fatty acid-binding protein (FABP4) was downregulated in the infected samples at both time points. This protein has recently been reported to be secreted by macrophages upon intracellular LPS-induced noncanonical inflammasome activation [69]. FABP4 is primarily expressed in adipocytes and macrophages. It binds to long-chain fatty acids and by this means can affect cellular lipid metabolism. *C. pneumoniae* has shown to recruit FABP4 to facilitate fat mobilization and intracellular growth in adipocytes [65]. Chemical inhibition of FABP4 decreases the intracellular replication of *C. pneumoniae* in murine adipocytes, and the *C. pneumoniae* infection induces FABP4 secretion in these cells [70]. It is tempting to speculate whether the decrease in intracellular FABP4 concentration in human macrophages upon *C. pneumoniae* infection results from its increased secretion. In macrophages, FABP4 has shown to affect fatty acid metabolism and inflammatory activity [71]. Genetic or chemical Inhibition of FABP4 also increased the expression of CD36. Of note, this scavenger receptor protein was also upregulated in our analysis as presented above.

Both at 48-h and 72-h postinfection, six out of the 10 most downregulated proteins were related to cell cycle control and DNA replication. Minichromosome maintenance (MCM) complex proteins MCM-6 were downregulated with fold changes of over -1.5 at both time points. The MCM2–7 complex acts as the eukaryotic replicate helicase and has a key role in the regulation of DNA replication [72]. The connection of some viruses and cancer types with MCM proteins has been studied during the last decade [73, 74], but its role in intracellular bacterial infections is currently unknown. Based on pathway analyses, replication protein, A 70 kDa DNA-binding subunit (RPA1) protein, was also found to accompany the MCM proteins in the network of DNA replication control proteins. In addition, protein mono-ADP-ribosyltransferase (PARP)10 was downregulated at 72-h postinfection. PARP10 regulates DNA replication via direct interactions with proliferating cell nuclear antigen [75], inhibits NF-κB signaling by interacting with the ubiquitylation of NF-κB essential modulator, NEMO [76], and alters mitochondrial function and fatty acid oxidation [77].

Generally, more proteins downregulated by the *C. pneumoniae* infection were identified at the latter 72-h time point than at 48-h postinfection, whereas the number of upregulated proteins was similar between the two time points.

3.4.3. C. pneumoniae Downregulates MCM Proteins in Differentiated Cells. Similar to the transcriptomics study in U937 monocytes [24], the most downregulated proteins in

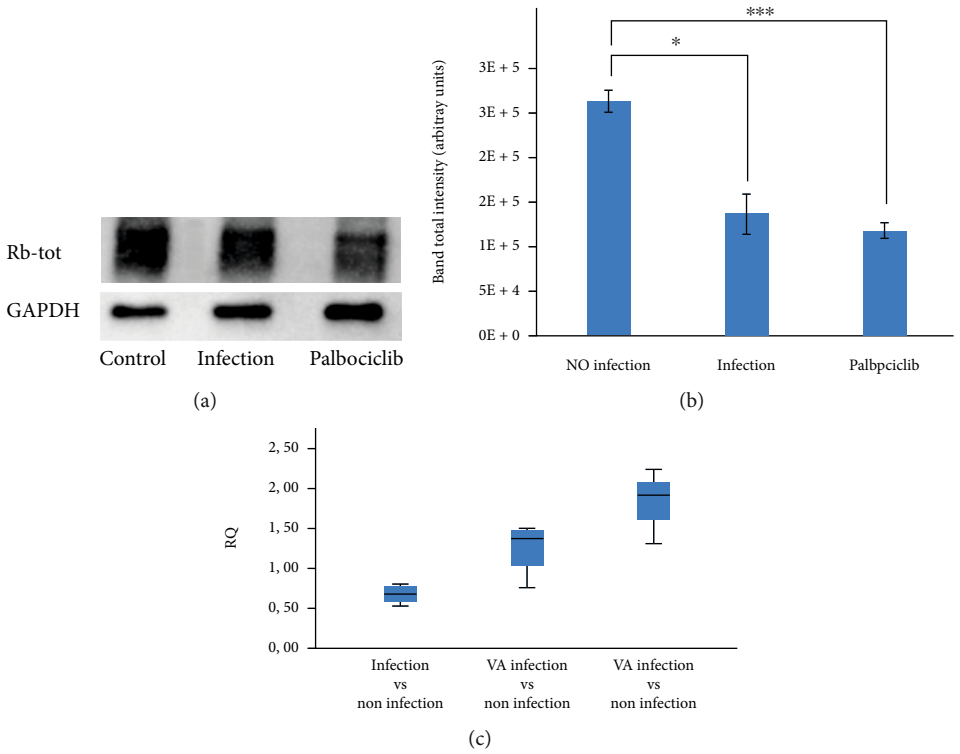

FIGURE 6: (a) Impact of *C. pneumoniae* infection on total retinoblastoma protein levels in THP-1 macrophages. Cells were infected with MOI 3 IFU/cell, and 100 nM Palbociclib was used as a control. Total cell lysate samples were collected at 48-h postinfection, and the total Rb levels of the samples was determined by western blot using polyclonal rabbit IgG antibody. GAPDH was used as a loading control. (b) Quantification of the Rb protein band intensities. The western blot band intensities were normalized to the total protein content of corresponding lane. The blots were analyzed using ChemiDoc imaging system and ImageLab 6.0 software (Bio-Rad). Data are shown as total intensity of band ± SEM ($n = 4$) in arbitrary units. (c) Changes in the expression of retinoblastoma gene mRNA levels induced by infection or valproic acid. Total RNA of the cells were collected at 48-h postinfection. After cDNA synthesis, the expression of each gene was determined by $2^{-\Delta\Delta Ct}$ method using GADPH as an internal reference gene ($n = 4$). Differences between means were calculated with Student's t-test with Bonferroni correction. Statistical analysis was made by IBM SPSS statistics 25 software. Statistical significance is presented as marks of p values: < 0.05:∗; <0.01: ∗∗; <0.001: ∗∗∗. Abbreviations: VA = valproic acid; Rb=retinoblastoma; Rq = relative quantification; Infection= mock-treated infection.

our data were related to cell cycle control and cellular proliferation. While we found all six members of the MCM protein family (MCM 2-7) downregulated by the infection, the U937 transcriptomics study found the sole MCM 7 to be strongly downregulated in U937 monocytes.

In contrast to Virok et al., we used THP-1 cells induced to growth arrest and terminal differentiation by PMA treatment. The 72-h PMA treatment prior to infection induces growth arrest at G1 stage of the cell cycle, a step preceding DNA replication. Opposite to freely dividing monocytes, the cells undergoing terminal differentiation to macrophages are expected to have low MCM protein levels. It was thus somewhat surprising that the levels were further decreased by the infection. Since changes in the host cell proteome can be caused by alterations in mRNA production or later by various downstream processes, the origin of the infection-induced lowering of MCM proteins was studied by determining the mRNA levels of the MCM genes by RT-PCR. Cyclin-dependent kinase 6 (CDK6) was also included in these analyses, as this cell cycle regulator acts upstream from MCM proteins and showed a downregulated trend at the protein level (Supplementary information Table 3). Corresponding to the proteomic findings, the expression of all MCM proteins showed moderate downregulation in the infected cells (Figure 5). The CDK6 mRNA was also downregulated by the infection. MCM 4 ($p = 0.027$) and CDK6 ($p = 0.01$) showed also statistical significance between infected and noninfected samples.

3.4.4. C. pneumoniae Infection Downregulates Retinoblastoma Gene and Protein in THP-1 Macrophages. Since the abundance of MCM proteins was significantly lower in infected vs. noninfected samples, and the transcript levels of the genes were correspondingly decreased, it was of interest to study the upstream events resulting to this phenomenon. The classic model of MCM gene transcriptional control involves sequestration of E2F transcription factors by retinoblastoma (Rb), where Rb phosphorylation leads to E2F release [78]. In the cell cycle G1 state, Rb protein phosphorylation is mediated by cyclin-dependent kinases and especially by CDK4/6.

As described above, CDK6 appeared in our study to be downregulated at both transcriptional (Figure 5) and protein levels (supplementary Table 3), although the latter change

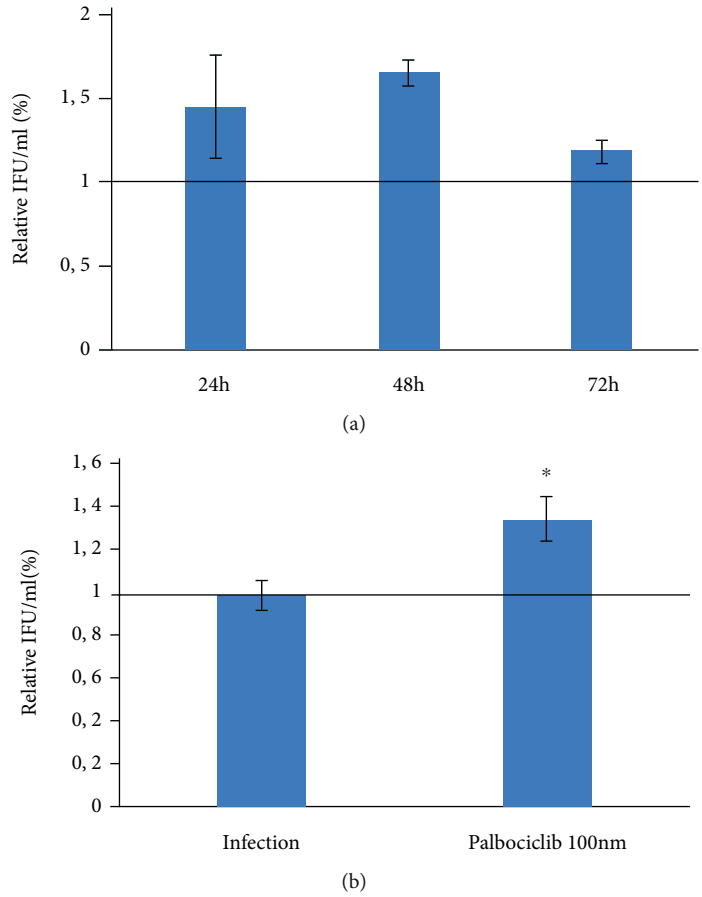

Figure 7: Impact of CDK4/6 inhibition on *C. pneumoniae* growth. (a) *C. pneumoniae* growth kinetics in THP-1 macrophages treated with 100 nM Palbociclib. Cells were infected at MOI 1 IFU/cell, and *C. pneumoniae* genome copy numbers were determined by qPCR on ompA gene. Data are shown as total genome numbers of *C. pneumoniae* per well normalized to nontreated infection control ± SEM ($n = 4$). Statistical significance was not noticed by *t*-test. (b) Impact of Palbociclib treatment on infectious *C. pneumoniae* EB production in THP-1 macrophages. The macrophages were infected with MOI 1 of *C. pneumoniae* and treated with 100 nM Palbociclib for 72 h before lysing. Permissive epithelial cells were inoculated with the macrophage lysates. *C. pneumoniae* inclusion counts were determined by immunofluorescence staining of the monolayers and converted to IFU/ml. Data are presented as IFU/ml values normalized to the value 72 h mock-treated infection and shown as mean ± SEM ($n = 4$). Statistical analysis was made by IBM SPSS statistics 25 software. Differences between means were calculated with Student's *t*-test with Bonferroni correction. Statistical significance is presented as marks of *p*-value: <0.05:∗.

did not reach statistical significance (fold change 0.71 and 0.72 at 48-h and 72-h postinfection, respectively). However, The THP-1 cells used as the infection host were induced to G1/S arrest in the cell cycle by PMA prior infection. The PMA-induced cell cycle arrest is mediated by Rb hypophosphorylation via p21 upregulation and subsequent CDK2 inactivation [79]. Consistent with these data, Rb phospho-ser780 antibody did not yield any signal in western blot analysis of THP-1 macrophages either in infected or noninfected cells, and Rb phospho-ser608-specific antibody yielded only a very faint signal (data not shown). Given the evident Rb hypophosphorylation in even uninfected THP-1 cells, it is obvious that the infection-induced downregulation of MCM proteins is not mediated by the inhibition of Rb phosphorylation.

Unexpectedly, the western blot analysis revealed an infection-induced decrease in total retinoblastoma protein level in THP-1 macrophages (Figures 6(a) and 6(b)). We confirmed the infection-induced Rb downregulation also in mRNA level with RT-PCR. In this analysis, the downregulation of the Rb gene by *C. pneumoniae* infection was observed with RQ value 0.43 (SEM = 0,011, *p*-value 0.054).

3.4.5. C. pneumoniae Infection Induces Myeloid-Derived Suppressor Cell (MDSC)-Like Changes in THP-1 Macrophages. The maintenance of high Rb levels is required for the maturation of monocyte lineage cells, and Rb is also involved in the terminal differentiation of these cells via direct interactions with tissue-specific genes [80]. Rb downregulation in *C. pneumoniae*-infected cells may thus indicate altered differentiation of the cells. In fact, the silencing of Rb protein in myeloid cells has previously been connected to the altered maturation of monocytes into polymorphonuclear myeloid-derived suppressor cells (PM-MDSC) instead of macrophages or dendritic cells [81]. The Rb downregulation in this context is related to epigenetic regulation and is

reversible by histone deacetylase inhibition. To evaluate the mechanisms of *C. pneumoniae*-induced Rb downregulation in THP-1 cells, the impact of a histone deacetylase inhibitor, valproic acid on Rb1 mRNA expression in *C. pneumoniae*-infected cells was studied. While the infection consistently downregulated Rb mRNA in this experiment, treatment of the infected cells with 1 mM valproic acid reversed the Rb expression closer to the levels observed in noninfected control cells (RQ value 1.86, SEM 0.19, between VA-treated and nontreated infection, $n = 4$), yet no statistical significance was achieved due to inter-experiment variability in the delta Ct values (Figure 6(c)). Together with the negative regulation of the sirtuin pathway identified in the proteomics data, these findings imply that *C. pneumoniae* may alter the epigenetic signature of macrophages. Earlier work has identified *Chlamydia*-induced changes in histone modifications and chromatin accessibility in permissive epithelial and endothelial cells [82, 83], but the significance of such changes for chlamydial survival and infection phenotype remains unknown.

MDSCs are a heterogenous group of myeloid cells with potent immune regulatory activity to negatively regulate T-cell function [84]. They are associated with failure in tumor clearance by the immune system but have also been indicated in the pathogenesis of chronic inflammatory diseases. Within the development of the pathologically immature phenotype of MDSCs, the upregulation of S100A8 and S100A9 plays a central role, via mechanisms involving reactive oxygen species (ROS) production [74]. In our proteomics data, S100A8 and S100A9 were among the most upregulated proteins (Table 1), and we have earlier reported the elevation of ROS by *C. pneumoniae* in the same infection model [29]. Another molecular mechanism of MDSC immunosuppressive function is the activation of noncanonical NF-κB signaling [85], which was also indicated by our proteomics data based on the infection-induced upregulation of NF-κB p100 (NF-κB2) (Table 1).

Collectively, the upregulation of S100A8, S100A9, and NF-κB p100 (NFKB2) and the downregulation of Rb, potentially involving an epigenetic mechanism, imply that *C. pneumoniae* infection may induce myeloid cells to a MDSC-like transformation. More detailed characterization of such events and their potential role in the maintenance of persistent *C. pneumoniae* infections remains a matter of our future studies.

3.4.6. CDK6 Inhibition Promotes C. pneumoniae Productive Infection. Alterations in host cell cycle regulation by *C. pneumoniae* have been described also in earlier work. However, it remains unclear whether such changes have a role in chlamydial survival and/or replication. To shed light on the significance of G1/S cell cycle arrest signals on *C. pneumoniae* infection phenotype in THP-1 macrophages, we treated infected cells with Palbociclib, a clinically approved CDK4/6 inhibitor. As presented in Figure 7, Palbociclib treatment increased chlamydial genome copy numbers by 1.66-fold (t-test p-value 0.053) compared to nontreated control infection at 48-h postinfection.

In addition, infectious *C. pneumoniae* EB progeny was significantly (1.32-fold) increased compared to nontreated controls. Thus, the inhibition of CDK6 activity promoted both bacterial replication and the maturation of new EBs, indicating that the suppression of G1 to S transition observed by us and others is relevant for promoting the productive chlamydial infection.

Earlier work on *C. pneumoniae*–host interactions has revealed the enhanced proliferation of infected cells, particularly in vascular cell types [86]. However, the cell type-specific nature of the mitogenic effects has been well acknowledged, and in monocyte lineage cells, the infection has been associated with growth arrest rather than increased proliferation. Referring to the work by Yamaguchi et al. [20], *C. pneumoniae* infection is often mentioned to induce monocytes to macrophage maturation. Based on the data presented in the current work, this may represent an oversimplified view. The THP-1 cells used in the current study were induced to differentiate with 72-h treatment with PMA prior to *C. pneumoniae* infection. As described by Daigneault et al. [38], this treatment induces gene expression changes similar to primary monocyte to macrophage differentiation within the days following PMA removal. The noninfected cells of the current study represent a similar situation, whereas the *C. pneumoniae*-infected cells seem to undergo altered differentiation. This is characterized at least by the infection-induced upregulation of CD14 and TLR2 (Table 1) and the alterations associated with the MDSC phenotype discussed above.

4. Conclusions

Monocytes and macrophages represent key cell populations in chlamydial persistence due to the antibiotic-refractory nature of the infection in these cells. They also have an important role in disseminating the pathogen from the respiratory tract to secondary sites of infection. The current work sheds light on the macrophage responses *regular front C. pneumoniae* infection at the proteome level, revealing the prominent upregulation of proinflammatory cascades and alterations in host cell cycle regulation pathways. Our data indicates that *C. pneumoniae* infection alters macrophage differentiation and disturbs the expression of host cell G1 stage-associated signaling molecules. Based on the growth-promoting effect of the CDK4/6 inhibitor, such changes favor chlamydial survival and progeny production in macrophages undergoing terminal differentiation.

Data Availability

The proteomics data used to support the findings of this study have been deposited to the ProteomeXchange Consortium via the PRIDE [1] partner repository with the dataset identifier PXD030232 and are also included within the supplementary information files of this article.

Conflicts of Interest

The authors declare that no conflicts of interest exist.

Acknowledgments

The work has been financially supported by Academy of Finland grant 333291 to LH and Finnish Cultural Foundation grant to ETW. Mass spectrometry-based proteomic analyses were performed by the Proteomics Core Facility, Department of Immunology, University of Oslo/Oslo University Hospital, which is supported by the Core Facilities program of the South-Eastern Norway Regional Health Authority. This core facility is also a member of the National Network of Advanced Proteomics Infrastructure (NAPI), which is funded by the Research Council of Norway INFRASTRUKTUR-program (project number: 295910).

Supplementary Materials

Supplementary Figure 1. Graphical summary on *C. pneumoniae*-induced signaling pathways in THP-1 macrophages at 48-h and 72-h postinfection. Orange = positively affected; blue = negatively affected. The analysis was carried out with Ingenuity Pathway Analysis (see Materials and methods for details). Supplementary Figure 2 Impact of *C. pneumoniae* infection on NFKB2 and S100A9 protein levels in THP-1 macrophages. Cells were infected with MOI 3 IFU/cell, and 100 nM Palbociclib was used as a control. Total cell lysate samples were collected at 48-h and 72-h postinfection, and protein levels of the samples was determined by western blot using polyclonal rabbit IgG antibody. GAPDH was used as inner control. Supplementary Table 1 Primers used in RT-PCR analysis. Supplementary Table 2 Label-free quantitations of the identified proteins ($n = 2136$). Supplementary Table 3. A one-way ANOVA (permutation-based FDR 0.10) identified differentially expressed proteins in *C. pneumoniae*-infected macrophages ($n = 214$). Numbers of LFQ fold change are presented as results from pairwise comparisons with Student's t-test. *(Supplementary Materials)*

References

[1] C. Kuo, R. S. Stephens, P. M. Bavoil, and B. Kaltenboeck, "Chlamydia," *Bergey's Manual of Systematics of Archaea and Bacteria*, pp. 1–28, 2015.

[2] A. Khoshbayana, F. Taherib, M. T. Moghadama, Z. Chegini, and A. Shariati, "The association of Chlamydia pneumoniae infection with atherosclerosis: review and update of in vitro and animal studies," *Microbial Pathogenesis*, vol. 154, p. 104803, 2021.

[3] W. C. Webley and D. L. Hahn, "Infection-mediated asthma: etiology, mechanisms and treatment options, with focus on Chlamydia pneumoniae and macrolides," *Respiratory research*, vol. 18, no. 1, p. 98, 2017.

[4] S. Grieshaber, N. Grieshaber, H. Yang, B. Baxter, T. Hackstadt, and A. Omsland, "The impact of active metabolism on Chlamydia trachomatis elementary body transcript profile and infectivity," *Journal of Bacteriology*, vol. 200, no. 14, 2018.

[5] M. E. Panzetta, R. H. Valdivia, and H. A. Saka, "Chlamydia persistence: a survival strategy to evade antimicrobial effects in-vitro and in-vivo," *Frontiers in Microbiology*, vol. 9, 2018.

[6] F. Njaua, R. Geffers, J. Thalmann, H. Haller, and A. D. Wagner, "Restriction of Chlamydia pneumoniae replication in human dendritic cell by activation of indoleamine 2,3-dioxygenase," *Microbes and Infection*, vol. 11, no. 13, pp. 1002–1010, 2009.

[7] S. P. Ouellette, T. P. Hatch, Y. M. AbdelRahman, L. A. Rose, R. J. Belland, and G. I. Byrne, "Global transcriptional upregulation in the absence of increased translation in chlamydia during IFNγ-mediated host cell tryptophan starvation," *Molecular Microbiology*, vol. 62, no. 5, pp. 1387–1401, 2006.

[8] H. M. Al-Younes, T. Rudel, V. Brinkmann, A. J. Szczepek, and T. F. Meyer, "Low iron availability modulates the course of Chlamydia pneumoniae infection," *Cellular Microbiology*, vol. 3, no. 6, pp. 427–437, 2001.

[9] L. G. Pantoja, R. D. Miller, J. A. Ramirez, R. E. Molestina, and J. T. Summersgill, "Characterization of Chlamydia pneumoniae persistence in HEp-2 cells treated with gamma interferon," *Infection and Immunity*, vol. 69, no. 12, pp. 7927–7932, 2001.

[10] J.-A. Herweg and T. Rudel, "Interaction of Chlamydiae with human macrophages," *The FEBS Journal*, vol. 283, no. 4, pp. 608–618, 2016.

[11] J. Rupp, L. Pfleiderer, C. Jugert et al., "Chlamydia pneumoniae hides inside apoptotic neutrophils to silently infect and propagate in macrophages," *Plos One*, vol. 4, no. 6, article e6020, 2009.

[12] A. Klos, J. Thalmann, J. Peters, H. C. Gérard, and A. P. Hudson, "The transcript profile of persistent Chlamydophila (Chlamydia) pneumoniae in vitro depends on the means by which persistence is induced," *FEMS Microbiology Letters*, vol. 291, no. 1, pp. 120–126, 2009.

[13] J. Peters, S. Hess, K. Endlich et al., "Silencing or permanent activation: host-cell responses in models of persistent Chlamydia pneumoniae infection," *Cellular Microbiology*, vol. 7, no. 8, pp. 1099–1108, 2005.

[14] M. Eickhoff, J. Thalmann, S. Hess et al., "Host cell responses to Chlamydia pneumoniae in gamma interferon-induced persistence overlap those of productive infection and are linked to genes involved in apoptosis, cell cycle, and metabolism," *Infection and Immunity*, vol. 75, no. 6, pp. 2853–2863, 2007.

[15] L. Mannonen, E. Kamping, T. Penttilä, and M. Puolakkainen, "IFN-g induced persistent Chlamydia pneumoniae infection in HL and Mono Mac 6 cells: characterization by real-time quantitative PCR and culture," *Microbial Pathogenesis*, vol. 36, no. 1, pp. 41–50, 2004.

[16] A. Marangoni, C. Bergamini, R. Fato et al., "Infection of human monocytes by Chlamydia pneumoniae and Chlamydia trachomatis: an in vitro comparative study," *BMC Research Notes*, vol. 7, no. 1, p. 230, 2014.

[17] C. Lim, C. J. Hammond, S. T. Hingley, and B. J. Balin, "Chlamydia pneumoniae infection of monocytes in vitro stimulates innate and adaptive immune responses relevant to those in Alzheimer's disease," *Journal of Neuroinflammation*, vol. 11, no. 1, p. 217, 2014.

[18] M. G. Netea, C. H. Selzman, B. J. Kullberg et al., "Acellular components of Chlamydia pneumoniae stimulate cytokine production in human blood mononuclear cells," *European Journal of Immunology*, vol. 30, no. 2, pp. 541–549, 2000.

[19] N. Takaoka, L. A. Campbell, A. Lee, M. E. Rosenfeld, and C. C. Kuo, "Chlamydia pneumoniae infection increases adherence of mouse macrophages to mouse endothelial cells in vitro and to aortas ex vivo," *Infection and Immunity*, vol. 76, no. 2, pp. 510–514, 2008.

[20] H. Yamaguchi, S. Haranaga, R. Widen, H. Friedman, and Y. Yamamoto, "Chlamydia pneumoniae infection induces differentiation of monocytes into macrophages," *Infection and Immunity*, vol. 70, no. 5, pp. 2392–2398, 2002.

[21] D. Flego, M. Bianco, A. Quattrini et al., "Chlamydia pneumoniae modulates human monocyte-derived dendritic cells functions driving the induction of a Type 1/Type 17 inflammatory response," *Microbes and Infection*, vol. 15, no. 2, pp. 105–114, 2013.

[22] M. Kortesoja, E. Taavitsainen, and L. Hanski, "The influence of dibenzocyclooctadiene lignans on macrophage glutathione and lipid metabolism associated with Chlamydia pneumoniae-induced foam cell formation," *Advances in Redox Research*, vol. 1, article 100001, 2021.

[23] G. Tumurkhuu, J. Dagvadorj, R. A. Porritt et al., "Chlamydia pneumoniae hijacks a host autoregulatory IL-1β loop to drive foam cell formation and accelerate atherosclerosis," *Cell Metabolism*, vol. 28, no. 3, pp. 432–448.e4, 2018.

[24] D. Virok, A. Loboda, L. Kari et al., "Infection of U937 monocytic cells with Chlamydia pneumoniae induces extensive changes in host cell gene expression," *The Journal of Infectious Diseases*, vol. 188, no. 9, pp. 1310–1321, 2003.

[25] C. Buccitelli and M. Selbach, "mRNAs, proteins and the emerging principles of gene expression control," *Nature Reviews Genetics*, vol. 21, no. 10, pp. 630–644, 2020.

[26] Y. Liu, A. Beyer, and R. Aebersold, "On the dependency of cellular protein levels on mRNA abundance," *Cell*, vol. 165, no. 3, pp. 535–550, 2016.

[27] K. Savijoki, J. Alvesalo, P. Vuorela, M. Leinonen, and N. Kalkkinen, "Proteomic analysis of Chlamydia pneumoniae-infected HL cells reveals extensive degradation of cytoskeletal proteins," *FEMS Immunology and Medical Microbiology*, vol. 54, no. 3, pp. 375–384, 2008.

[28] M. Kortesoja, R. E. Trofin, and L. Hanski, "A platform for studying the transfer of Chlamydia pneumoniae infection between respiratory epithelium and phagocytes," *Journal of Microbiological Methods*, vol. 171, p. 105857, 2020.

[29] E. Taavitsainen, M. Kortesoja, T. Bruun, N. G. Johansson, and L. Hanski, "Assaying Chlamydia pneumoniae persistence in monocyte-derived macrophages identifies Dibenzocyclooctadiene Lignans as phenotypic switchers," *Molecules*, vol. 25, no. 2, p. 294, 2020.

[30] M. Johnson, I. Irena Zaretskaya, Y. Raytselis, Y. Merezhuk, S. McGinnis, and T. L. Madden, "NCBI BLAST: a better web interface," *Nucleic Acids Research*, vol. 36, no. Web Server, pp. W5–W9, 2008.

[31] K. Shima, M. Wanker, R. J. Skilton et al., "The genetic transformation of Chlamydia pneumoniae," *mSphere*, vol. 3, no. 5, pp. e00412–e00418, 2018.

[32] S. Tyanova, T. Temu, P. Sinitcyn et al., "The Perseus computational platform for comprehensive analysis of (prote)omics data," *Nature Methods*, vol. 13, no. 9, pp. 731–740, 2016.

[33] D. Szklarczyk, A. L. Gable, D. Lyon et al., "STRING v11: protein-protein association networks with increased coverage, supporting functional discovery in genome-wide experimental datasets," *Nucleic Acids Research*, vol. 47, no. D1, pp. D607–D613, 2019.

[34] C. A. Gaydos, J. T. Summersgill, N. N. Sahney, J. A. Ramirez, and T. C. Quinn, "Replication of Chlamydia pneumoniae in vitro in human macrophages, endothelial cells, and aortic artery smooth muscle cells," *Infection and Immunity*, vol. 64, no. 5, pp. 1614–1620, 1996.

[35] S. Haranaga, H. Yamaguchi, H. Ikejima, H. Friedman, and Y. Yamamoto, "Chlamydia pneumoniae infection of alveolar macrophages: a model," *The Journal of Infectious Diseases*, vol. 187, no. 7, pp. 1107–1115, 2003.

[36] K. Wolf, E. Fischer, and T. Hackstadt, "Degradation of chlamydia pneumoniae by peripheral blood monocytic cells," *Infection and Immunity*, vol. 73, no. 8, pp. 4560–4570, 2005.

[37] T. Buchacher, A. Ohradanova-Repic, H. Stockinger, M. B. Fischer, and V. Weber, "M2 polarization of human macrophages favors survival of the intracellular pathogen chlamydia pneumoniae," *PLoS One*, vol. 10, no. 11, article e0143593, 2015.

[38] M. Daigneault, J. A. Preston, H. M. Marriott, M. K. Whyte, and D. H. Dockrell, "The identification of markers of macrophage differentiation in PMA-stimulated THP-1 cells and monocyte-derived macrophages," *PLoS One*, vol. 5, no. 1, article e8668, 2010.

[39] L. Hanski, D. Ausbacher, T. M. Tiirola, M. B. Strøm, and P. M. Vuorela, "Amphipathic β2,2-amino acid derivatives suppress infectivity and disrupt the intracellular replication cycle of Chlamydia pneumoniae," *PLoS One*, vol. 11, no. 6, article e0157306, 2016.

[40] P. Matzneller, S. Krasniqi, M. Kinzig et al., "Blood, tissue, and intracellular concentrations of azithromycin during and after end of therapy," *Antimicrobial Agents and Chemotherapy*, vol. 57, no. 4, pp. 1736–1742, 2013.

[41] M. Ashburner, C. A. Ball, J. A. Blake et al., "Gene Ontology: tool for the unification of biology," *Nature Genetics*, vol. 25, no. 1, pp. 25–29, 2000.

[42] The Gene Ontology Consortium Author Notes, "The Gene Ontology resource: enriching a gold mine," *Nucleic Acids Research*, vol. 49, no. D1, pp. D325–D334, 2021.

[43] S.-H. Lee, J.-H. Lee, H.-Y. Lee, and K.-J. Min, "Sirtuin signaling in cellular senescence and aging," *BMB Reports*, vol. 52, no. 1, pp. 24–34, 2019.

[44] G.-J. Zhao, Z.-C. Mo, S.-L. Tang et al., "Chlamydia pneumoniae negatively regulates ABCA1 expression via TLR2-nuclear factor-kappa B and miR-33 pathways in THP-1 macrophage-derived foam cells," *Atherosclerosis*, vol. 235, no. 2, pp. 519–525, 2014.

[45] C. P. da Costa, C. J. Kirschning, D. Busch et al., "Role of chlamydial heat shock protein 60 in the stimulation of innate immune cells by Chlamydia pneumoniae," *European Journal of Immunology*, vol. 32, no. 9, pp. 2460–2470, 2002.

[46] G. Miao, X. Zhao, B. Wang et al., "TLR2/CXCR4 coassociation facilitates Chlamydia pneumoniae infection-induced atherosclerosis," *American Journal of Physiology-Heart and Circulatory Physiology*, vol. 318, no. 6, pp. H1420–H1435, 2020 Jun 1.

[47] J. Németh, I. Stein, D. Haag et al., "S100A8 and S100A9 are novel nuclear factor kappa B target genes during malignant progression of murine and human liver carcinogenesis," *Hepatology*, vol. 50, no. 4, pp. 1251–1262, 2009.

[48] K. Hsu, Y. M. Chung, Y. Endoh, and C. L. Geczy, "TLR9 ligands induce S100A8 in macrophages via a STAT3-dependent pathway which requires IL-10 and PGE2," *PLoS One*, vol. 9, no. 8, article e103629, 2014.

[49] S. Wang, R. Song, Z. Wang, Z. Jing, S. Wang, and J. Ma, "S100A8/A9 in inflammation," *Frontiers in Immunology*, vol. 9, p. 1298, 2018.

[50] C. H. Sunderkötter, J. Tomimori-Yamashita, V. Nix et al., "High expression of myeloid-related proteins 8 and 14 characterizes an inflammatorily active but ineffective response of macrophages during leprosy," *Immunology*, vol. 111, no. 4, pp. 472–480, 2004.

[51] X. Zou, B. S. Sorenson, K. F. Ross, and M. C. Herzberg, "Augmentation of epithelial resistance to invading bacteria by using mRNA transfections," *Infection and Immunity*, vol. 81, no. 11, pp. 3975–3983, 2013.

[52] G. Assadi, L. Vesterlund, F. Bonfiglio et al., "Functional analyses of the Crohn's disease risk gene LACC1," *PLoS One*, vol. 11, no. 12, article e0168276, 2016.

[53] A. Lahiri, H. Hedl, J. Yan, and C. Abraham, "Human LACC1 increases innate receptor-induced responses and a LACC1 disease-risk variant modulates these outcomes," *Nature Communications*, vol. 8, no. 1, p. 15614, 2017.

[54] M. A. Icer and M. Gezmen-Karadag, "The multiple functions and mechanisms of osteopontin," *Clinical Biochemistry*, vol. 59, pp. 17–24, 2018.

[55] D. P. NyströmT and A. Hultgårdh-Nilsson, "A constitutive endogenous osteopontin production is important for macrophage function and differentiation," *Experimental Cell Research*, vol. 313, no. 6, pp. 1149–1160, 2007.

[56] S. A. Steitz, M. Y. Speer, G. Curinga et al., "Smooth muscle cell phenotypic transition associated with calcification: upregulation of Cbfa1 and downregulation of smooth muscle lineage markers," *Circulation Research*, vol. 89, no. 12, pp. 1147–1154, 2001.

[57] A. Rizzo, C. R. Carratelli, A. D. Filippis, N. Bevilacqua, M. A. Tufano, and E. Buommino, "Transforming activities of Chlamydia pneumoniae in human mesothelial cells," *International Microbiology*, vol. 17, no. 4, pp. 185–193, 2014.

[58] C. Wahl, F. Oswald, U. Simnacher, S. Weiss, R. Marre, and A. Essig, "Survival of Chlamydia pneumoniae-infected Mono Mac 6 cells is dependent on NF-κB binding activity," *Infection and Immunity*, vol. 69, no. 11, pp. 7039–7045, 2001.

[59] O. V. Savinova, A. Hoffmann, and G. Ghosh, "The Nfkb1 and Nfkb2 proteins p105 and p100 function as the core of high-molecular-weight heterogeneous complexes," *Molecular Cell*, vol. 34, no. 5, pp. 591–602, 2009.

[60] S.-C. Sun, "The non-canonical NF-κB pathway in immunity and inflammation," *Nature Reviews Immunology*, vol. 17, no. 9, pp. 545–558, 2017.

[61] S. O. Rahaman, D. J. Lennon, M. Febbraio, E. A. Podrez, S. L. Hazen, and R. L. Silverstein, "A CD36-dependent signaling cascade is necessary for macrophage foam cell formation," *Cell Metabolism*, vol. 4, no. 3, pp. 211–221, 2006.

[62] W. Liu, P. He, B. Cheng, C. Mei, Y. Wang, and J. Wan, "Chlamydia pneumoniae disturbs cholesterol homeostasis in human THP-1 macrophages via JNK-PPARγ dependent signal transduction pathways," *Microbes and Infection*, vol. 12, no. 14-15, pp. 1226–1235, 2010.

[63] L. Törmäkangas, L. Erkkila, T. Korhonen et al., "Effects of repeated Chlamydia pneumoniae inoculations on aortic lipid accumulation and inflammatory response in C57BL/6J mice," *Infection and Immunity*, vol. 73, no. 10, pp. 6458–6466, 2005.

[64] K. Bloom, A.-W. Mohsen, A. Karunanidhi et al., "Investigating the link of ACAD10 deficiency to type 2 diabetes mellitus," *Journal of Inherited Metabolic Disease*, vol. 41, no. 1, pp. 49–57, 2018.

[65] N. F. Walenna, Y. Kurihara, B. Chou et al., "Chlamydia pneumoniae exploits adipocyte lipid chaperone FABP4 to facilitate fat mobilization and intracellular growth in murine adipocytes," *Biochemical and Biophysical Research Communications*, vol. 495, no. 1, pp. 353–359, 2018.

[66] A. K. Bachhawat and S. Yadav, "The glutathione cycle: glutathione metabolism beyond the γ-glutamyl cycle," *IUBMB Life*, vol. 70, no. 7, pp. 585–592, 2018.

[67] A. A. Azenabor and A. U. Chaudhry, "Chlamydia pneumoniae survival in macrophages is regulated by free Ca2+ dependent reactive nitrogen and oxygen species," *The Journal of Infection*, vol. 46, no. 2, pp. 120–128, 2003.

[68] A. A. Azenabor, K. Muili, J.-F. Akoachere, and A. Chaudhry, "Macrophage antioxidant enzymes regulate Chlamydia pneumoniae chronicity: evidence of the effect of redox balance on host-pathogen relationship," *Immunobiology*, vol. 211, no. 5, pp. 325–339, 2006.

[69] M. B. Lorey, K. Rossi, K. K. Eklund, T. A. Nyman, and S. Matikainen, "Global characterization of protein secretion from human macrophages following non-canonical Caspase-4/5 inflammasome activation," *Molecular & Cellular Proteomics*, vol. 16, no. 4, pp. S187–S199, 2017.

[70] N. F. Walenna, Y. Kurihara, B. Chou, K. Ishii, T. Soejima, and K. Hiromatsu, "Chlamydia pneumoniae infection–induced endoplasmic reticulum stress causes fatty acid–binding protein 4 secretion in murine adipocytes," *The Journal of Biological Chemistry*, vol. 295, no. 9, pp. 2713–2723, 2020.

[71] L. Makowski, K. C. Brittingham, J. M. Reynolds, J. Suttles, and G. S. Hotamisligil, "The fatty acid-binding protein, ap2, coordinates macrophage cholesterol trafficking and inflammatory activity, macrophage expression of ap2 impacts peroxisome proliferator-activated receptor γ and iκb kinase activities," *The Journal of Biological Chemistry*, vol. 280, no. 13, pp. 12888–12895, 2005.

[72] T. D. Deegan and J. F. Diffley, "MCM: one ring to rule them all," *Current Opinion in Structural Biology*, vol. 37, pp. 145–151, 2016.

[73] D. P. Malinowski, "Molecular diagnostic assays for cervical neoplasia: emerging markers for the detection of high-grade cervical disease," *BioTechniques*, vol. 38, no. 4S, p. S17, 2005.

[74] J. Zheng, "Diagnostic value of MCM2 immunocytochemical staining in cervical lesions and its relationship with HPV infection," *International Journal of Clinical and Experimental Pathology*, vol. 8, no. 1, pp. 875–880, 2015.

[75] E. M. Schleicher, A. M. Galvan, Y. Imamura-Kawasawa, G. L. Moldovan, and C. M. Nicolae, "PARP10 promotes cellular proliferation and tumorigenesis by alleviating replication stress," *Nucleic Acids Research*, vol. 46, no. 17, pp. 8908–8916, 2018.

[76] P. Verheugd, A. H. Forst, L. Milke et al., "Regulation of NF-κB signalling by the mono-ADP-ribosyltransferase ARTD10," *Nature Communications*, vol. 4, no. 1, p. 1683, 2013.

[77] J. Márton, T. Fodor, L. Nagy et al., "PARP10 (ARTD10) modulates mitochondrial function," *PLoS One*, vol. 13, no. 1, article e0187789, 2018.

[78] Y. J. Choi and L. Anders, "Signaling through cyclin D-dependent kinases," *Oncogene*, vol. 33, no. 15, pp. 1890–1903, 2014.

[79] K. Traore, M. A. Trush, M. George Jr., E. W. Spannhake, W. Anderson, and A. Asseffa, "Signal transduction of phorbol 12-myristate 13-acetate (PMA)-induced growth inhibition of

human monocytic leukemia THP-1 cells is reactive oxygen dependent," *Leukemia Research*, vol. 29, no. 8, pp. 863–879, 2005.

[80] G. Bergh, M. Ehinger, I. Olsson, S. E. Jacobsen, and U. Gullberg, "Involvement of the retinoblastoma protein in monocytic and neutrophilic lineage commitment of human bone marrow progenitor cells," *Blood*, vol. 94, no. 6, pp. 1971–1978, 1999.

[81] J.-I. Youn, V. Kumar, M. Collazo et al., "Epigenetic silencing of retinoblastoma gene regulates pathologic differentiation of myeloid cells in cancer," *Nature Immunology*, vol. 14, no. 3, pp. 211–220, 2013.

[82] R. J. Hayward, J. W. Marsh, M. S. Humphrys, W. M. Huston, and G. S. A. Myers, "Chromatin accessibility dynamics of Chlamydia-infected epithelial cells," *Epigenetics & Chromatin*, vol. 13, no. 1, p. 45, 2020.

[83] B. Schmeck, W. Beermann, P. D. N'Guessan et al., "Simvastatin reduces Chlamydophila pneumoniae-mediated histone modifications and gene expression in cultured human endothelial cells," *Circulation Research*, vol. 102, no. 8, pp. 888–895, 2008.

[84] V. Bronte, S. Brandau, S.-H. Chen et al., "Recommendations for myeloid-derived suppressor cell nomenclature and characterization standards," *Nature communications*, vol. 7, no. 1, 2016.

[85] J. Yu, Y. Wang, F. Yan et al., "Noncanonical NF-κB activation mediates STAT3-stimulated IDO upregulation in myeloid-derived suppressor cells in breast cancer," *Journal of Immunology*, vol. 193, no. 5, pp. 2574–2586, 2014.

[86] J. M. Kern, V. Maass, and M. Maass, "Molecular pathogenesis of chronic Chlamydia pneumoniae infection: a brief overview," *Clinical Microbiology and Infection*, vol. 15, no. 1, pp. 36–41, 2009.